Nuclear Instruments and Methods in Physics Research A 661 (2012) S121–S124

Contents lists available at ScienceDirect

Nuclear Instruments and Methods in Physics Research A

journal homepage: www.elsevier.com/locate/nima

The CBM time-of-flight wall

I. Deppner [a,*], N. Herrmann [a], D. Gonzalez-Diaz [b], V. Ammosov [c], J. Cheng [d], M. Ciobanu [b], V. Gapienko [c], K.D. Hildenbrand [b], A. Kiseleva [b], M. Kiš [b], D. Kresan [b], R. Kotte [e], C. Huangshan [d], Y. Leifels [b], J. Fruehauf [b], C. Li [b], Y. Li [d], P.-A. Loizeau [a], L. Naumann [e], M. Petrovici [g], M. Petris [g], A. Semak [c], V. Simion [g], D. Stach [e], Y. Sun [f], Yu. Sviridov [c], Z. Tang [f], E. Usenko [c], J. Wang [d], Y. Wang [d], K. Wisniewski [a], J. Wüstenfeld [e], L. Xu [f], V. Zaets [c], Y. Zhang [a], X. Zhu [d]

[a] Physikalisches Institut Uni. Heidelberg, Heidelberg, Germany
[b] GSI, Darmstadt, Germany
[c] IHEP, Protvino, Moscow Region, Russia
[d] Tsinghua University, Beijing, China
[e] FZ Dresden-Rossendorf, Dresden, Germany
[f] USTC, Hefei, China
[g] NIPNE, Bucharest, Romania

ARTICLE INFO

Available online 7 October 2010

Keywords:
CBM
Time-of-flight
RPC
Semi-conductive glass
Cross-talk
Multi-strip
High rate

ABSTRACT

The key element providing hadron identification in the future Compressed Baryonic Matter spectrometer at FAIR is a time-of-flight wall placed at 10 m distance from the target. The most promising technological option for such a task consists on a 150 m^2 carpet based on Resistive Plate Chambers. Due to the fixed-target geometry, the conceptual design foresees two extreme regions: an outermost region (low rate/low multiplicity) covered by float glass RPCs in multi-strip fashion, and a central region (high rate/high multiplicity) consisting of densely packed read-out cells made with low resistive electrodes. The status of the ongoing R&D efforts in both regions is presented.

1. Introduction

The Compressed Baryonic Matter (CBM) spectrometer will be operational in year 2017 at the Facility for Anti-proton and Ion Research (FAIR) in Darmstadt, Germany. The spectrometer aims at systematically studying rare and bulk probes stemming from heavy ion reactions in the energy regime 2–90 A GeV, in order to precisely characterize the phase diagram of nuclear matter and eventual first or second order phase-transitions [1]. The most important tool providing hadron identification is a time-of-flight (ToF) wall placed at 10 m from the target, with a polar angular coverage of 2.5– 25° and full azimuth. According to simulations, separating pions, kaons and protons up to few GeV/c momentum requires of a ToF resolution of 80 ps at high efficiency, while the cell occupancy must be kept down to $\simeq 5\%$. The differential study of rare probes (importantly J/Ψ and Ψ' through di-lepton decay) imposes an interaction rate as high as 10 MHz for the system Au+Au at 25 A GeV. Such a luminosity yields a particle flux of around 20 kHz/cm^2 in the central region of the ToF wall, falling nearly exponentially down to 500 Hz/cm^2 in the outermost region (Fig. 1). A design occupancy of 5% for the most central collisions in the aforementioned system (75 000 readout channels) leads, similarly, to very different counter granularities in both regions: 4–6 cm^2 and 250 cm^2, respectively. On one hand, this fact enforces the choice of a strip layout for the outermost part. On the other hand, the high channel density in the central part imposes naturally the development of low-power and compact Front End Electronics, desirably at ASIC level.

2. The CBM ToF wall

Resistive Plate Chambers with sub-mm gas gaps in multi-gap structures [2,3] are so far the best technological choice that fulfills the CBM-ToF wall requirements. Its conceptual design foresees an array of 80 super-modules (SM) with a active area of 1.5 m × 1 m each. These SMs are mechanically arranged along nine columns and form four concentric so-called 'rate regions' (Figs. 2 and 3). The RPCs from the central super-modules have thus to cope with particle fluxes between 8 and 25 kHz/cm^2 with granularities in the range of 4–6 cm^2. Not being accessible to state-of-the-art timing RPCs, these fluxes seem to be well within reach for a next generation of counters thanks to the development of glass with low-resistivity $\rho_{20} = 3 \times 10^{10}\ \Omega$ cm, hereafter called 'Chinese

* Corresponding author.
E-mail address: deppner@physi.uni-heidelberg.de (I. Deppner).

0168-9002/$ - see front matter © 2010 Elsevier B.V. All rights reserved.
doi:10.1016/j.nima.2010.09.165

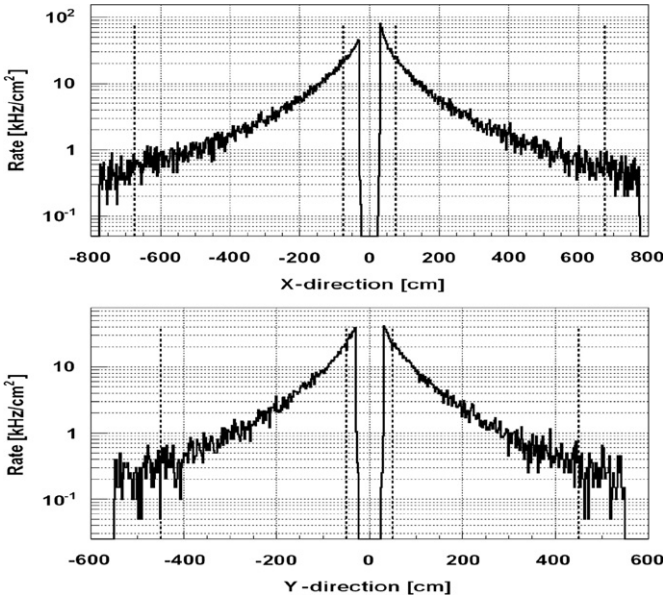

Fig. 1. Simulated particle flux over the CBM ToF wall in x and y direction for the highest expected rate of Au+Au collisions at 25 A GeV. The x axis is the direction of the magnetic field kick. The vertical dashed lines represent the detector acceptance.

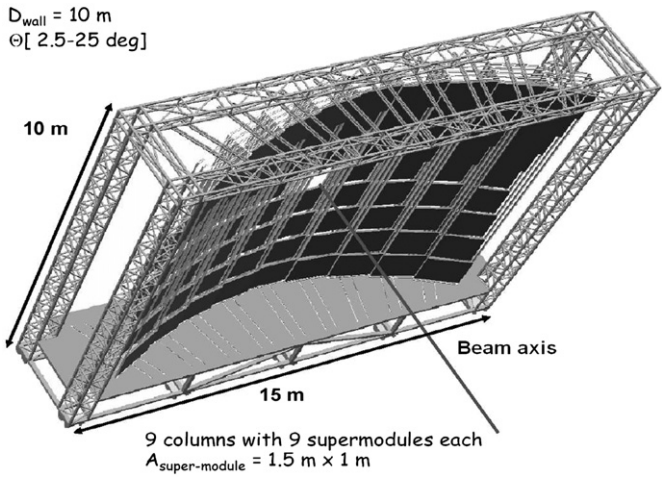

Fig. 2. Base-line ToF wall engineering design.

glass' [5]. This new material exhibits a highly ohmic behavior, very low dark currents and rates once assembled in the counter, high stability of operation and low carrier loss for a total transported charge density of up to 1 C/cm^2.[1]

The segmentation of the SMs in smaller modules seems unavoidable, specially in the central region, where 2500–3500 channels will be distributed among ~ 100 modules, for a total of 8 SMs. Rate regions 2 and 3, not accessible by standard float glass RPCs, require a channel density of approximately 1250 and 750 ch/SM for a total of 12 and 16 SMs, respectively. The largest part of the ToF wall (44 SMs) has to deal with an average rate below 1 kHz/cm^2 and will be thus covered by RPCs made out of float glass. Based on previous encouraging studies [6], an additional moderate detector warming ($\Delta T \simeq 10^{\circ}$) may be used if necessary in order to increase the rate

[1] This figure corresponds to the charge transported by counters in the central region, for 2 years operation under AuAu collisions at 25 A GeV and full luminosity, assuming $\overline{q} \simeq 1$ pC average avalanche charge per gap.

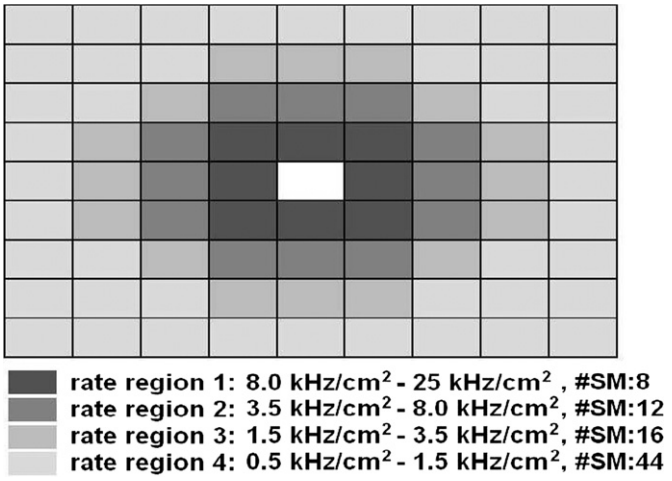

Fig. 3. Particle load on the 80 super-modules, separated in four regions with similar flux.

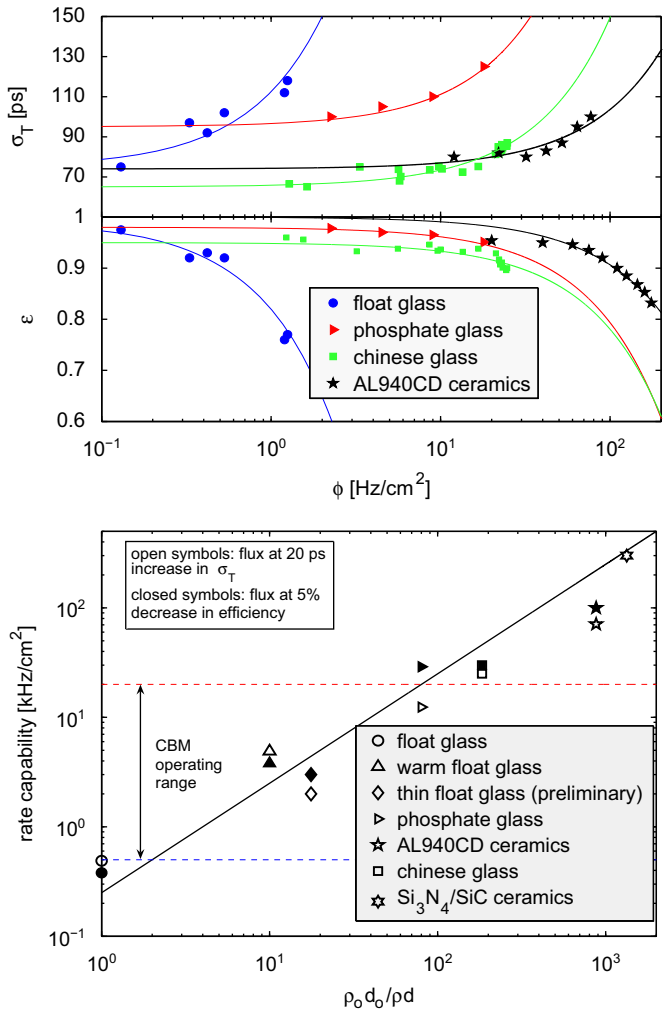

Fig. 4. Up: behavior of efficiency and resolution as a function of the particle flux for [4] (○), [8] (right △), [5] (□) and [7] (⋆) together with a linear fit. Down: measured rate capability (maximum operating flux) as a function of $1/\rho d$ for various counters, [4] (○), [6] (△), [12] (◇), [8] (right △), [7] (⋆), [5] (□) and [11] (6-peak ⋆).

capability (△ in Fig. 4, for $\Delta T \simeq 25^{\circ}$). The use of multi-strip layouts with lengths 15–150 cm for covering regions 2–4 is a practical imposition due to the very large area involved (90% of the total).

Dedicated simulations/measurements have been carried out in order to ensure both low cross-talk and the necessary signal integrity for preserving the time resolution.

3. High rate capability prototypes

An R&D program aimed at pushing the rate capability of timing RPCs above 20 kHz/cm^2 has yielded various sensitive developments (most notably [5–8]). At present, the efforts are focused on consolidating the various options in real-size modules, with a channel density similar to the final one. Two of these concepts have been presented at this workshop: (i) a 10 gap differential RPC in a double stack configuration with 250 μm gap size based on Chinese glass [9]. The counter has an active area of 13 cm × 4.2 cm and is subdivided in twelve 2 cm × 2 cm pads with an interval (separation between pads) of 2 mm; (ii) a second type of module with similar dimensions (18 cm × 4.6 cm) but a much higher granularity (72 × 2 channels) is at present being tested in-beam [10]. The strip width is 1.1 and 0.34 mm the interval. The same number of gaps (10) but with a thickness of only 140 μm is used, being read-out also differentially. Prototypes with both Pestov and Chinese glass have been developed in this variant.

Recent developments on ceramics (in particular SiN_2/SiC composites) are pushing the RPC rate capability on the verge of 1 MHz/cm^2 [11]. These materials offer the desirable possibility of 'adjusting' the bulk resistivity in the range 10^7-10^{12} Ω cm, depending on the needs. The varistor-type electrical behavior (strongly non-ohmic) and a lack of scheme for industrial production are still open questions for long-term production, but steps are being taken in that direction.

At last, an 'ad hoc' solution for CBM would consist on single-pad RPCs made of commercially available ultra-thin glass (0.17 mm and lower) warmed up by 20–30°. This solution possibly represents a practical upper limit to the rate capability of float glass-based RPCs, and is being currently explored [12].

3.1. Systematics on rate capability

There is abundant experimental evidence supporting the fact that the main limitation of the RPC performances at high particle fluxes stems mainly from the average current $\bar{I}$ produced by the avalanches (DC model). Under the assumptions stated in [13], the following simple expressions for the time resolution σ_T and efficiency ε, can be obtained for moderate particle fluxes:

$$\sigma_T = \sigma_0 + K_T \bar{q} \phi \rho d \quad (1)$$

$$\varepsilon = \varepsilon_0 - K_\varepsilon \bar{q} \phi \rho d \quad (2)$$

where d is the average plate thickness per gap and K_T, K_ε are positive constants depending on the RPC multi-gap structure. This functional dependence has been used to fit some published data in Fig. 4 upper panel.

The second term in Eqs. (1) and (2) determines how much the performances deteriorate for a given particle flux ϕ. Thus, it is reasonable to expect that a differential deterioration of performances scales linearly with $\bar{q}\phi\rho d$. Operatively, the rate capability is here defined as the particle flux for which a resolution deterioration by 20 ps or a 5% efficiency drop is observed (open and closed symbols in Fig. 4, respectively). The rate capability is plot as a function of $1/\rho d$ for various CBM prototypes, normalized to the typical value in float glass RPCs ($\rho_0 d_0 = 300$ GΩ cm^2). The scaling in Fig. 4 lower panel adds extra support to the 'DC model' image for these counters, although counter-to-counter structural differences add considerable scattering with respect to the ideal scaling.

Transient [13,14] and non-uniformity [15] effects are expected to be small for the measurements here compiled, so that the rate capability resembles much the one expected in conditions of uniform and stationary irradiation where Eqs. (1) and (2) hold, and under which the detectors are expected to run. For details the reader is referred to the corresponding publications.

4. Multi-strip prototypes

Addressing the multi-hit capabilities of multi-strip counters is of utmost importance. High cross-talk and loss of signal integrity is expected for long counters, if proper precautions are not taken [16]. Complementary, a strip segmentation bigger than a typical avalanche foot-print of ~7 mm is desired in order to minimize the number of required channels, by keeping a cluster size close to one. Several counters with lengths in the range D=240–1000 mm and widths w=7–25 mm have been built based on standard float glass technology layered out over 8–12 gaps, and a detailed analysis will be published elsewhere.

The counters are evaluated mainly on the basis of position scans across the strips, where the avalanche footprint is responsible for a higher cluster size in the region between strips, and cross-talk is determined as a flat background for positions far from that region. A typical distribution together with preliminary simulations (following Ref. [16]) is shown in Fig. 5. Overall, the observed cross-talk is well below 3%, at efficiencies higher or around 90%. Optimization of cross-talk and signal integrity relies, so far, on relatively large strip to strip intervals or guard walls.

Multi-hit performances have been preliminary evaluated, showing a moderate degradation of the time resolution when a (second) coincident track arrives simultaneously at one of the strip first neighbors.

4.1. Differential and matched counter

A new type of detector has been presented at the workshop. The design is genuinely differential (anode and cathode have the same electrostatic coupling). The strip width is kept at the level of 7 mm with 3 mm interval, designed to provide a low strip to strip

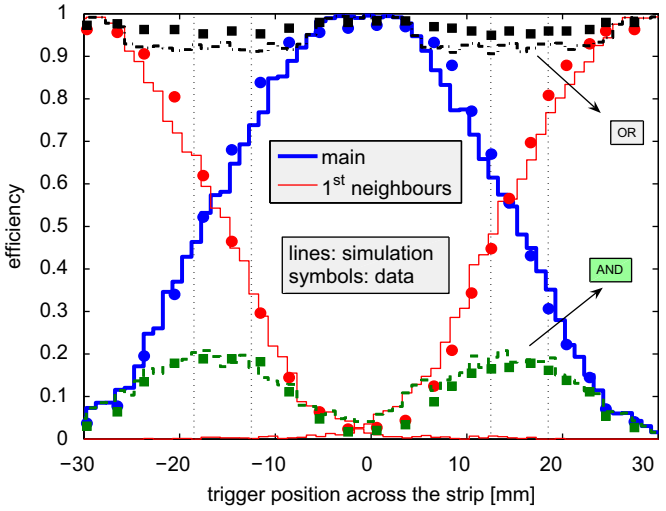

Fig. 5. Preliminary efficiency as a function of the position across the strip for a 50 cm long counter under a low-resolution analysis (2 cm wide trigger). Circles show the measured probability of the central strip (simulation: thick line) or any of the neighbors (simulation: thin line) to fire. Squares show the measured probability that any of the three strips fire (simulation: dot-dashed) and that the central and any of the neighbors do (simulation: dashed).

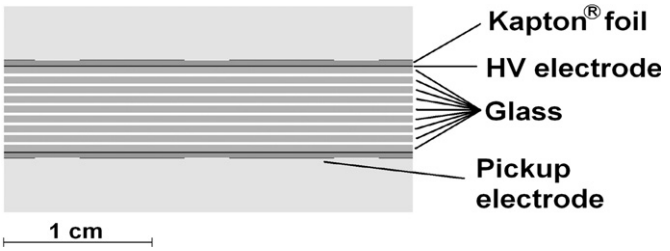

Fig. 6. Layout of the differential and impedance matched counter ($Z_{diff} \sim 2 \times 50\,\Omega$) developed at Heidelberg.

coupling and guarantee an overall differential impedance close to $Z_c \simeq 100\,\Omega$. Neglecting back-coupling from the first neighbor strips (ideal ground) and considering only coupling between opposing strips, a differential impedance $Z_{diff} = 2(Z_c - Z_m) = 86\,\Omega$ was determined with the APLAC HF-simulator [17], reasonably matching the observed one by time-domain reflectometry measurements. A differential impedance close to $100\,\Omega$ is a desirable feature, since a $2 \times 50\,\Omega$ pseudo-differential front-end electronics has been developed by the CBM-ToF group, integrated in the PreAmplifier-DIscriminator ASIC PADI [18]. An optimized impedance yields higher signal transmission and increases the system stability.

The active area of the prototype (Fig. 6) is 28 cm $\times$ 16.5 cm. Its active volume is subdivided in 8 gaps by nine 0.55 mm thick float glass plates. The gas gap is ensured by 220 μm thick fishing lines. The bottom and top plates are covered by conductive layers ($R \simeq 10\,M\Omega/\square$) that serve for HV distribution. The two outermost FR-4 plates provide a substrate for the electrode manufacturing as well as the required mechanical stiffness. Additional cross-talk optimization can be easily performed after detector mounting by fine adjustment of those plates thickness.

5. Conclusions

An RPC rate capability at the level of 20 kHz/cm^2, as required for the central part of the CBM-ToF wall, together with long-term stability of the plate properties has been demonstrated for low-conductive glasses, but several new materials are at present close to these benchmarks as well.

For the outermost part of the wall (low granularity/low rate), several multi-strip modules have been tested up to 1 m length showing very modest cross-talk levels of 2–3% at an efficiency above 90%.

With the R&D phase almost finished, the CBM-ToF group is now focusing on the development of the first real-scale detector modules.

Acknowledgements

The work was supported in part by BMBF project 06HD9121I, by the EU-FP7 WP2 and by HIC for FAIR.

References

[1] P. Senger, et al., J. Phys. G 36 (2009) 064037.
[2] E. Cerron Zeballos, et al., Nucl. Instr. and Meth. A 374 (1996) 132.
[3] P. Fonte, et al., Nucl. Instr. and Meth. A 443 (2000) 201.
[4] D. Gonzalez-Diaz, Ph.D., J. Instr. TH003 (2006).
[5] J. Wang, et al., Nucl. Instr. and Meth. A 621 (2010) 151.
[6] D. Gonzalez-Diaz, et al., Nucl. Instr. and Meth. A 555 (2005) 72.
[7] L. Lopes, et al., Nucl. Phys. B (Proc. Suppl.) 158 (2006) 66.
[8] A. Akindinov, et al., Nucl. Instr. and Meth. A 572 (2007) 676.
[9] J. Wang, et al., Progress of R & D and production of timing RPCs in Tsinghua University, this issue, doi:10.1016/j.nima.2010.08.076.
[10] M. Petris, et al., Toward a high granularity and high counting rate, differential readout timing MRPC, this issue, doi:10.1016/j.nima.2010.09.162.
[11] L. Naumann, et al., High-rate timing RPC with ceramics electrodes, this issue, doi:10.1016/j.nima.2010.09.121.
[12] V. Ammosov, Beam test of pad tRPCs with ultra thin glass, talk at XIII CBM meeting, Darmstadt, 2009.
[13] D. Gonzalez-Diaz, et al., Nucl. Phys. B (Proc. Suppl.) 158 (2006) 111.
[14] P. Colrain, et al., Nucl. Instr. and Meth. A 456 (2000) 62.
[15] J. Lamas-Valverde, Ph.D. Thesis, CERN/LAA 97-03, 1997.
[16] D. Gonzalez-Diaz, Simulation of resistive plate chambers with multi-strip readout, this issue, doi:10.1016/j.nima.2010.09.067.
[17] 〈http://web.awrcorp.com/Usa/Products/APLAC/〉.
[18] M. Ciobanu, et al., IEEE NSS, Dresden, 2008.